Nanophotonics 1 (2012): 155–169 © 2012 Science Wise Publishing & De Gruyter • Berlin • Boston. DOI 10.1515/nanoph-2012-0012

Review

Nanowire-based plasmonic waveguides and devices for integrated nanophotonic circuits

Hong Wei and Hongxing Xu*

Beijing National Laboratory for Condensed Matter Physics and Institute of Physics, Chinese Academy of Sciences, Box 603-146, Beijing 100190, China, e-mail: hxxu@iphy.ac.cn

*Corresponding author

Abstract

The fast development of plasmonics have greatly advanced our understanding to the abundant phenomena related to surface plamon polaritons (SPPs) and improved our ability to manipulate light at the nanometer scale. With tightly confined local field, SPPs can be transmitted in waveguides of subwavelength dimensions. Nanophotonic circuits built with plasmonic elements can be scaled down to dimensions compatible with semiconductor-based nanoelectronic circuits, which provides a potential solution for the next-generation information technology. Different structures have been explored as plasmonic waveguides for potential integration applications. This review is focused on metallic nanowire waveguides and functional components in nanowire networks. We reviewed recent progress in research about plasmon generation, emission direction and polarization, group velocity, loss and propagation length, and the near-field distribution revealed by quantum dot fluorescence imaging. Electrical generation and detection of SPPs moves towards the building of plasmonic circuits, where bulky external light sources and detectors may be omitted. The coupling between metal nanowires and emitters is important for tailoring light-matter interactions, and for various potential applications. In multi-nanowire structures, plasmon signal control and processing are introduced. The working principles of these nanowire-based devices, which are based on the control to the near field distributions, will become the design rule for nanophotonic circuits with higher complexity for optical signal processing. The recent developments in hybrid photonic-plasmonic waveguides and devices are promising for making devices with unprecedented performance.

Keywords: surface plamon polaritons; nanowires; nanophotonic circuits.

1. Introduction

Photons as the information carriers have many advantages compared to electrons in speed, capacity and bandwidth as demonstrated in optical communications with optical fibers replacing copper wires, i.e., with photons replacing electrons as the information carriers. Photonic integrated circuits (ICs) have been widely used in fiber-optical communications, and biological and chemical sensing. Since electronic ICs based on semiconductors will soon reach the physical limit in speed as indicated by Moore's law, further miniaturization of optical ICs could make it a possible choice for future information processing and computing. However, the further miniaturization is limited by the diffraction limit of light in dielectric optical devices. Even with properly improved design, photonic ICs are usually believed to be only used in optical interconnection between electronic ICs, but with fundamental difficulties to be used for optical signal processing in ultra-compact ICs. With the advancement of nanofabrication techniques, metal nanostructures can be tailored with designed geometries. Gold and silver nanostructures show many unique properties based on the resonances of surface plasmon polaritons (SPPs), which are electromagnetic waves in metal-dielectric interfaces associated with collective oscillations of conduction-band electrons in metal [1]. The SPPs can concentrate electromagnetic energy at volumes on a nanometer scale, which enables the manipulation of light beyond the diffraction limit [2]. Therefore, SPPs can possibly enable highly dense integration of nanophotonic devices, and make it possible to design nanophotonic ICs based on SPPs for tomorrow's information technology. The studies related to SPPs have formed a booming field called plasmonics.

Depending on the plasmonic properties, metal nanostructures have been used in different fields. The SPP resonance frequencies depend strongly on the sizes and shapes of the nanostructures, and are sensitive to the change of the dielectric environment [3]. Based on the latter effect, sensing techniques using surface plasmon resonances (SPRs) and localized surface plasmon resonances (LSPRs) have been developed [4, 5]. Much effort has been devoted to exploring and designing nanostructures and experimental schemes to improve the detection sensitivity. Metal nanostructures can concentrate light energy in the vicinity of the structure and improve the intensity of the electromagnetic field around the structure. In coupled structures, such as a dimer of Au/Ag nanoparticles, the electric field is highly focused to the junction of the dimer [6, 7]. This largely enhanced electromagnetic field is the physical basis for many applications, including surface-enhanced spectroscopy [8], plasmon-assisted optical forces [9–11] and non-linear optics [12, 13]. Metal nanostructures have been used as antennas to manipulate the light transmission [14, 15]. Researchers have also employed plasmonic nanostructures for applications in cancer therapy [16], photovoltaic devices [17] and photocatalysis [18].

In metal films and one-dimensional nanostructures, SPPs propagate along the metal-dielectric interface over damping-restricted distances. Compared with dielectric optical fibers, one-dimensional plasmonic waveguides have a tightly confined electromagnetic field in the transverse direction. Therefore, more compact integration can be made by using plasmonic waveguides. As dielectric photonic devices have played an important role in the information processing field, the development of nanophotonics is required to make devices of nanoscale dimensions. With the advantage of subwavelength confinement, plasmonic components can be used to construct nanophotonic circuits, which interface with modern nanoelectronic devices. It is also possible to combine the transmission of optical and electric signals in one circuit, since the metal waveguides are electrically conductive. Therefore, SPP-involved nanophotonic circuits are promising for next-generation information technology.

One critical element to construct a plasmonic circuit is the plasmonic waveguide. Several different structures have been used as waveguides to transport surface plasmons of highly localized modes. Metal strips [19–21], wedges [22], grooves and slots in metal films [23–27], and dielectric strips on metal films [28, 29] have been investigated as plamonic waveguides. Crystalline metal nanowires, which are usually prepared by chemical methods, are another kind of waveguides. The plasmon damping during the propagation along the nanowire is lower due to the crystalline structure [30]. Therefore, the crystalline nanowires can support SPPs propagating over longer distances, and have been used in many studies to explore the surface plasmon guiding properties. These crystalline nanowires are easy to manipulate, and have been used to construct functional devices. In this review, we mainly focus on the waveguides based on metallic nanowires and functional components in simple nanowire networks.

2. Metallic nanowire waveguides

2.1. Conversion of photons to SPPs

Since the wavevector of surface plasmons is larger than that of light, the difference between the wavevectors has to be compensated to convert photons to surface plasmons. To launch the plasmons propagating in the nanowire, several excitation methods can be employed. A conventional configuration for exciting SPPs is the prism-coupled excitation in the Kretschmann-Raether configuration. This can be used to launch propagating plasmons in metal nanowire waveguides, as shown in Figure 1A. Both coherent and incoherent light sources can be used. If laser light is focused onto the tips of the nanowires, the scattering at the wire tip can also overcome the wavevector mismatch to launch the propagating plasmons (Figure 1B). Direct illumination on the midsection of the nanowire cannot excite the plasmons. However, if there is a defect on the wire or some nanoparticles attached to the wire, these discontinuous points can enable the conversion of photons into plasmons. Figure 1C shows a nanowire with a sharp kink. The laser light was focused on the position where

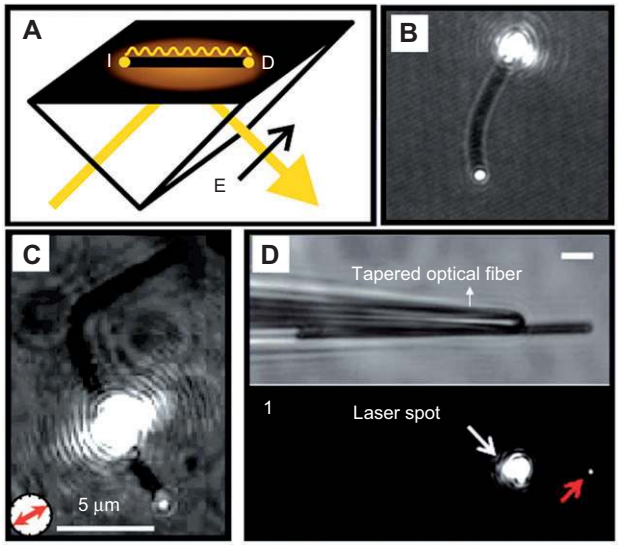

Figure 1 Optical excitation methods for surface plasmon polaritons propagating in metal nanowires [30–33].

a nanoparticle was adhered. The emission from the bottom tip of the nanowire indicates the generation of propagating plasmons. The kink itself provides an additional position to couple light into plasmons. Focusing the excitation light to the discontinuous points of the nanowire can easily be realized in experiments and is widely used in many studies.

Although direct far field illumination on the wire midsection cannot launch the SPPs, near field coupling between dielectric waveguide and the metal nanowire can excite the plasmons in the metal wire. Figure 1D shows a silver nanowire with a tapered optical fiber placed on top of it. The laser light travelled along the fiber to the fiber tip and coupled to SPPs in the silver nanowire, which was verified by the light emission at the right end of the wire marked by the red arrow.

Depending on the excitation geometry, the in-coupling efficiency for the conversion from light to plasmons varies. Antennas have been used to improve the in-coupling efficiency for plasmon excitation. In Figure 2A, a bowtie antenna is fabricated at the input end of a silver nanowire [34]. The near-field intensity at the points P and Q is measured by using a scanning near-field optical microscope (SNOM) system. The near-field intensity is increased when increasing the arm lengths of the antenna and reaches its maximum when the arm length is 250 nm (Figure 2B). Compared with the nanowire without the receiving antenna, the near-field intensity is enhanced, i.e., the in-coupling efficiency is improved, by a factor of 13.6. At the output end of the nanowire, a transmitting antenna can be fabricated. The transmitting antenna will enhance the out-coupling efficiency for the plasmon-photon conversion. For a Ag nanowire of about 100 nm diameter and 10 μm length with antennas at both input and output ends, the emission intensity is enhanced by a factor of 45, compared with a nanowire without any antenna. Theoretical investigations for improving the in-coupling efficiency by using aperture antenna and by engineering the nanowire cross-section have been reported in the literature [35, 36].

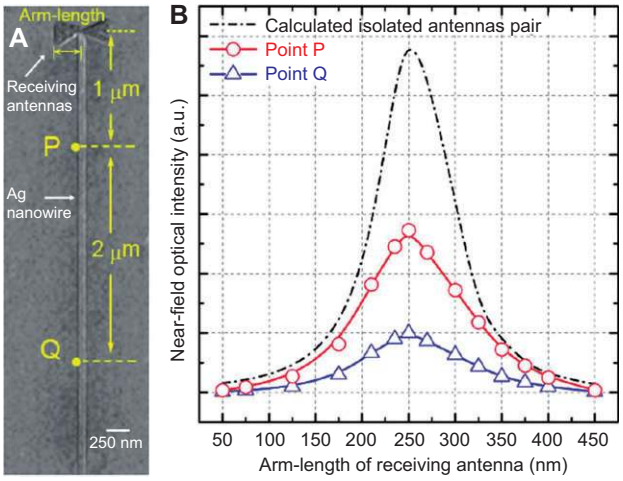

Figure 2 (A) Scanning electron microscopy (SEM) image of the top part of the 20 μm long Ag nanowire with one end placed at the feed gap of the receiving antenna pair. (B) Near-field intensity as a function of the arm length of the receiving antennas for an isolated bowtie antenna pair (calculated, black dash-dot line) and the equivalent positions P (experimental, red circles) and Q (experimental, blue triangles) with distances of 1 and 3 μm down from the bowtie, respectively. The maximum intensity is observed at an arm length of 250 nm [34].

2.2. Direction and polarization of emitted light

The propagating plasmons in metal nanowires will finally couple out as photons at the output terminal of the nanowire. For nanowires on supported glass substrates, in addition to the emission at the nanowire end, it is also possible to have emission into the optically dense substrate with a higher refractive index than the air on the top side of the nanowire. The emission into the glass substrates can be detected by using an oil immersion objective of high numerical aperture (NA). This method for SPP detection is usually called leakage radiation microscopy [37]. The angular distribution of the emission light intensity can be characterized by two spherical angles, θ and ϕ (Figure 3A) and can be directly imaged on the back focal plane of the objective [38]. The details about Fourier imaging can be found in the paper by Lieb et al. [39]. Fourier imaging has become a useful technique to study the directional properties in research of plasmonics [40–42]. Figure 3B shows the radiative emission of plasmons from the wire trunk and the end. By imaging the back focal plane of the objective with the excitation light blocked, the Fourier image is obtained as shown in Figure 3C. The Fourier image indicates that the surface plasmons in the nanowire emits with a narrow distribution for θ and ϕ. The emission directionality depends on both the refractive index of the media surrounding the nanowire and the thickness of the nanowire. Unidirectional emission is obtained for optically thick nanowires. The origin of the unidirectional radiation is examined by considering the radiation from oscillating dipoles. The radiation pattern from a chain of dipoles with internal phase retardation corresponding to a wave travelling in one direction, is quite similar to the experimentally obtained Fourier images. When the chain of dipoles oscillates, as if driven by two equal waves travelling in opposite directions, the unidirectionality is lost. The simulation result is consistent with the experiments for nanowires of different diameters. For a thick wire, the plasmons

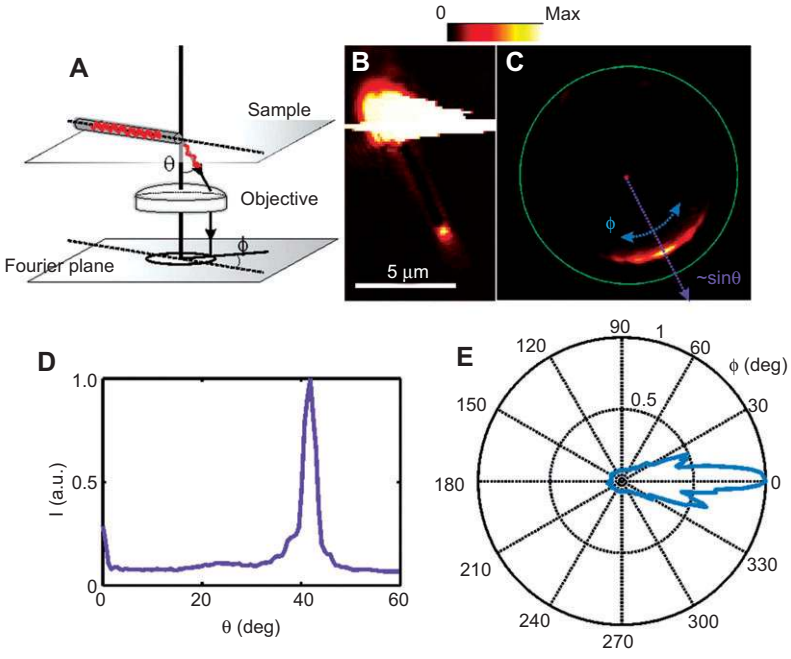

Figure 3 Unidirectional emission from a silver nanowire. (A) Illustration of the detection scheme and the coordinate system used. The nanowire is excited by a focused beam at the input end and the emitted light is detected in the Fourier plane of the optical microscope. (B) Direct optical image of a wire for λ=632.8 nm excitation. (C) Corresponding Fourier image with the incident light blocked by an aperture in the image plane. (D) Emission intensity vs. θ for ϕ=0 and (E) vs. ϕ for θ corresponding to maximum intensity [38].

travelling to the output end of the wire are mostly scattered out, with a very low intensity of plasmons reflected back. This one-directional travel guarantees unidirectional radiation. For a thin wire, part of the plasmons reaching the output end of the wire can be reflected and travel back, which destroys the unidirectionality and results in a more symmetric pattern.

The propagating plasmons in the metal nanowires are usually excited by light of a certain polarization. After transmitting through the nanowire in the form of plasmons and converted back to photons at the output end of the nanowire, whether the light emitted from the wire keeps the polarization state or not, is of considerable interests not only for fundamental research, but also for the applications in nanophotonic circuits for information transport. With different incident polarizations, two primary modes can be excited (more modes can be excited in thick wires), as shown in Figure 4A [43]. Light polarized parallel to the nanowire excites the m=0 mode with charge oscillations along the wire, while light polarized perpendicular to the nanowire excites the m=1 mode with charge oscillations perpendicular to the wire. The simulations for an ideal nanowire with flat facets at both ends show that, at parallel incident polarization, the wire keeps the polarization state, i.e., the emitted light is also polarized parallel to the wire (Figure 4B and 4C).

In experiments performed on nanowires on glass substrates covered by index-matching oil, both the nanowires maintaining polarization and rotating polarization are observed in measurements for different wires. Theoretical simulations show that the polarization state of the emitted light depends strongly on the shape of the nanowire terminals. The sensitivity to the terminal geometries can be understood by examining the in-coupling efficiency for photon-plasmon conversion and the damping length of the propagating plasmons. Figure 4D shows the in-coupling efficiency for the m=0 mode and m=1 mode. As can be seen, the in-coupling efficiency for the m=0 mode increases monotonically as the nanowire diameter decreases. For the m=1 mode, the in-coupling efficiency reaches a maximum for nanowires with a diameter of 120 nm. The damping length of both modes increases with the nanowire diameter. The geometries of input terminals of the nanowires determine the relative intensity of the two modes excited in the wire, and strongly influence the emission polarization. The shape of the output end influences the spatial distribution of the emitted light and also affects the emission polarization. If the nanowire end shapes can be tailored precisely, it is possible to selectively make nanowire waveguides that are either polarization-maintaining or polarization-rotating.

Theoretical studies reveal that the surface plasmons of the nanowire in a homogeneous medium propagate helically around the wire with the handedness (left- or right-hand twist) determined by the polarization of excitation light [44]. The chiral SPPs result in circularly polarized emission at the nanowire end in the near field regime (a vertical plane 200 nm

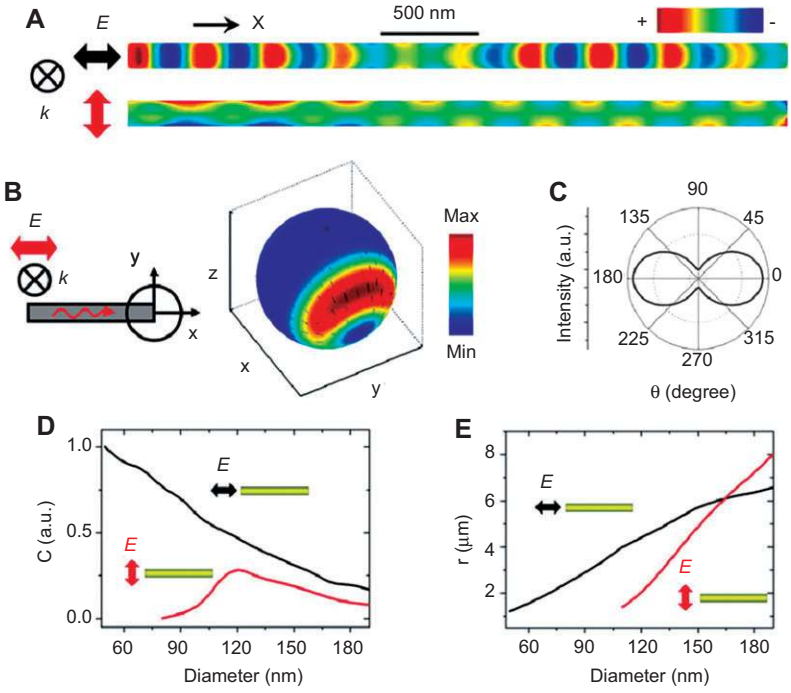

Figure 4 SPP modes in nanowires with flat terminations. (A) Charge distribution on the surface of a wire of the length 3.36 μm and diameter 130 nm, terminated by flat ends. The left end is excited by a 633 nm wavelength focused beam with polarization parallel and perpendicular to the wire, respectively. (B) The resulting spatial distribution of the emission intensity on a sphere enclosing the wire end excited by the parallel incident polarization. Colored and black lines represent the intensity and the polarization of the emission on the sphere. (C) Emission intensity of different polarizations from a wire excited under the parallel polarized excitation. (D) The in-coupling efficiency C for two SPP modes (black curve for m=0 mode, red curve for m=1 mode) as a function of the wire diameter. (E) The 1/e damping length, r, of both modes as a function of the wire diameter [43].

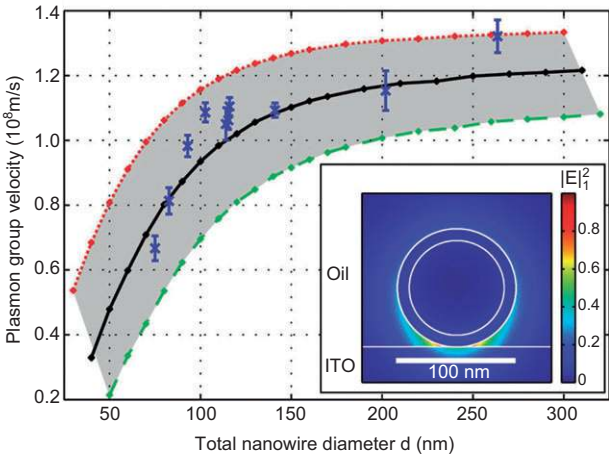

Figure 5 Plasmon group velocity as a function of the total nanowire diameter. Blue crosses indicate experimental results. Simulation results are represented by diamonds connected by lines. Results of simulations without a corrosion layer, a 5 nm, and a 10 nm corrosion layer of silver sulfide are indicated with red dotted and black and green dashed lines, respectively. Inset: Two-dimensional near-field intensity distribution of the fundamental plasmon mode for a silver nanowire, immersed in index-matched oil on a 200 nm thick ITO layer on top of glass. The nanowire diameter is d=100 nm including a 10 nm silver sulfide corrosion layer [47].

beyond the nanowire end mapped in the calculation). The high degree of circular polarization is maintained in a broad spectral band. Thus, metal nanowires can be used as a broadband sub-wavelength circularly polarized light source, which may find applications in nanophotonics.

2.3. Group velocity and propagation length

The difference of the dispersion relations for surface plasmons and light determines the group velocity difference between them. The group velocity of surface plasmons has been measured experimentally. Metal nanowires behave like a cavity and reflect part of the plasmons at the wire end depending on the wavelength. Thus the emission spectra of plasmons excited by broadband light show modulated intensity at different wavelengths. From the fringes in the spectra, the group velocity of plasmons can be deduced. The plasmon group velocity is around half that of light in vacuum and decreases with decreasing excitation wavelength [45, 46]. Rewitz et al. measured the plasmon group velocity for silver nanowires of different diameters using a spectral interferometry technique [47]. Their results show that the plasmon group velocity is decreased dramatically for nanowires with a diameter smaller than 100 nm (Figure 5). When the refractive index of the surrounding medium is increased, the group velocity is decreased.

During the propagation, the surface plasmons are partly dissipated due to nonradiative and radiative losses. This means that they can only propagate over certain distances. The plasmon damping length in silver nanowires is measured experimentally by exciting the plasmons at different positions on the wire by using a tapered optical fiber and record the emission intensity at the wire end [33, 48, 49]. The emission intensity at different excitation positions, i.e., propagating distances, can be fitted by an exponential decay function. The length at which the light intensity decreases to 1/e of the initial value is defined as the propagation length or damping length. From the above measured data, the propagation length can

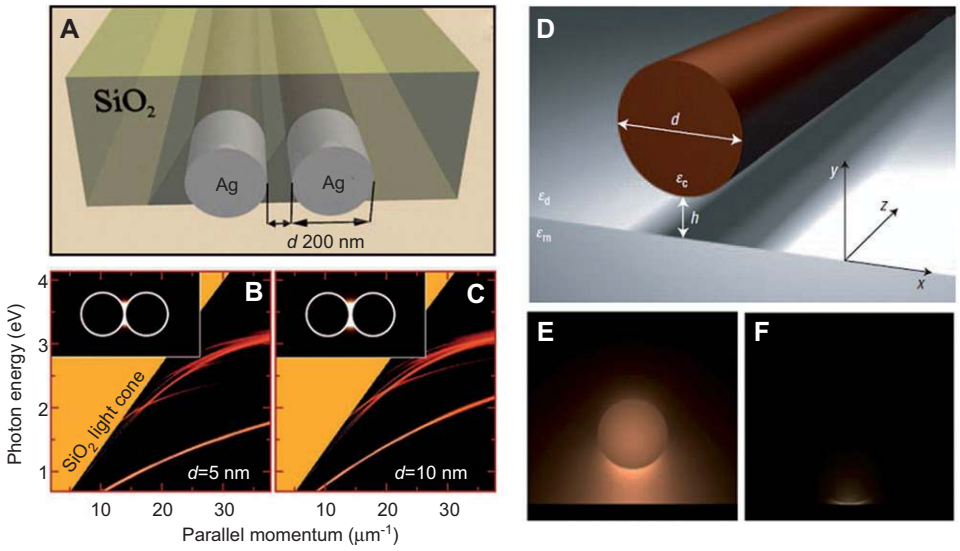

Figure 6 (A) Schematic view of the geometry for two parallel silver nanowires in silica. (B, C) Photonic density of states (DOS) as a function of energy and momentum parallel to the wires for different wire-pair separations *d*. The insets show the spatial distribution of the local density of states (LDOS) for the lowest-energy gap mode at a free-space light wavelength of 1550 nm. Brighter regions correspond to higher DOS and LDOS. The maximum LDOS in the inset of (C) is ~15000 times the vacuum value. (D) The hybrid optical waveguide. A semiconductor cylindrical nanowire of diameter d is separated from a silver half-space by a nanoscale dielectric gap. The nanowire is embedded in SiO_2. (E, F) Electromagnetic energy density distributions for [*d*, *h*]=[200, 100] nm and [200, 2] nm [53, 54].

be obtained. By coating the nanowire with fluorescent molecules, the emission intensity of plasmons excited by molecule fluorescence can also be used to measure the plasmon propagation length [50]. Solis et al. coated gold nanowires with a fluorescent polymer. By investigating the plasmon-induced bleaching of the polymer emission, the propagation length of plasmons in the gold wire was obtained [51].

If the nanowire is bent, the bending of the nanowire will cause an energy loss. Wang et al. used a micromanipulator to bend a silver nanowire to different curvatures and measured the loss caused by the nanowire bending [33]. By separating the propagation loss in a straight wire from the total loss, the pure loss by the bending is obtained. The bending loss is increased with an increase of the excitation light wavelength. For a fixed excitation wavelength, thicker wires suffer more bending losses.

The proximal substrate may cause additional damping of propagating plasmons in metal nanowires. Li et al. studied the effect of the silica layer on top of the silicon substrate on the plasmon propagation distance [52]. When the silica layer thickness is increased from 50 nm to 400 nm, the emission intensity at the nanowire end shows a non-monotonic behavior. The maximum intensity appears at a silica thickness of about 110 nm and 300 nm. Due to the reflection of the incident light from the silicon substrate, the interference of the incident light and reflected light will form a modulated electric field intensity distribution, which makes the in-coupling efficiency for the photon-plasmon conversion dependent on the silica layer thickness. The integrated contribution of the in-coupling efficiency and propagation length, which also depend on the silica layer thickness, results in an oscillation behavior of the emission intensity. When the silica layer is very thin, the plasmons are strongly damped by the proximal silicon substrate, which results in a very short propagation distance.

The balancing of field confinement and propagation length promotes attempts to design novel waveguide structures. Manjavacas and Garcia de Abajo proposed arrays of parallel metal nanowires for plasmon guiding [53]. The guiding mechanism relies on gap plasmons in the region between adjacent nanowire pairs and multiwire arrays. Figure 6A shows a nanowire pair embedded in silica. The relation between photon energy and momentum parallel to the wires, is shown for two different gap distances in Figure 6B and 6C. For a small wire separation, a strongly bound mode is observed, with a parallel momentum well above the momentum of light in the host silica (Figure 6B). This gap mode is tightly confined in the interwire region, which makes it interact weakly with other structures. On the other hand, the gap modes can propagate a considerable distance. To consider the tradeoff between propagation distance and mode confinement, the figure of merit (FOM) for the waveguides, defined as the ratio of the propagation distance and the geometric mean of the mode diameter in the transverse directions, can be compared. The FOM for a wire pair is larger than that of a single wire. Another kind of waveguide employing gap modes is the hybrid waveguide with a dielectric nanowire close to the top of a metal surface (Figure 6D), which was proposed by Oulton et al. [54]. The mode coupling between the nanowire and the metal surface results in a hybrid mode (Figure 6E). When the gap is decreased to the nanometer scale, the hybrid mode is strongly confined in the gap (Figure 6F). This gap mode enables electromagnetic energy transmission in the non-metallic region over long distances.

Theoretical research is performed in many groups to investigate properties of plasmons in metal nanowire waveguides [55–61]. Many efforts have been devoted to decreasing the plasmon loss and increasing the propagation length. Researchers have reported loss compensation in different plasmonic systems using different gain materials [62–74]. These efforts deepen our understanding of using gain media to compensate for plasmon loss, and will help to design plasmonic waveguides of lower energy damping.

2.4. Near-field distributions

When surface plasmons propagate along the nanowire, the near-field distribution can be detected by using scanning near-field optical microscopy (SNOM) [30]. The advantage of SNOM is the resolution beyond the diffraction limit of light [75]. If the nanowire waveguides are coated by fluorescent emitters, such as quantum dots or molecules, the intensity of plasmon-induced fluorescence is proportional to the local field intensity. Therefore, the fluorescence can be used to map the near-field intensity distribution. Compared with SNOM, the fluorescence imaging is diffraction-limited. However, it works much faster than SNOM and has much lower demand on the sample. Therefore, the fluorescence-based far-field imaging method is a useful tool for imaging the plasmon local field distribution on larger scale. Ditlbacher et al. used the fluorescence of Rhodamin 6G molecules to image the plasmon field profile on a metal film [76].

Figure 7 shows a silver nanowire of 300 nm diameter coated by a layer of semiconductor quantum dots (QDs) with 30 nm Al_2O_3 as a spacer between the silver wire and the QDs [77]. The fluorescence image in Figure 7ii, obtained by wide field excitation shows that the coating of QDs on the wire

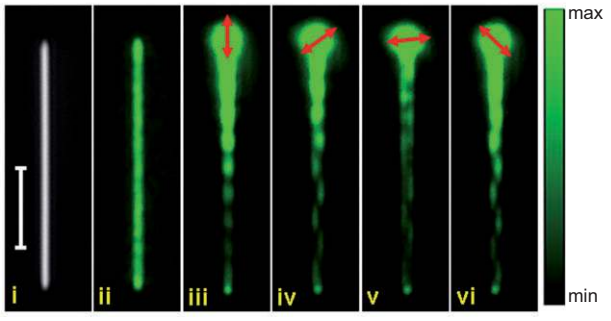

Figure 7 QD emission images of plasmons launched by 632.8 nm laser excitation at one end of a Ag nanowire. Changing the polarization angle at the input modifies the field distribution in the nanowire. (i) Optical image of a Ag nanowire. (ii) The QD emission image with wide field excitation. (iii–vi) QD emission images for different polarizations of the incident laser. The scale bar is 5 μm. The red arrows indicate the laser polarization [77].

is quite uniform and the fluorescence intensity is enhanced by the silver wire. A laser light of 633 nm wavelength was focused onto the top end of the nanowire to launch the propagating plasmons. The QDs on the wire were excited and emitted fluorescence. A modulated quasi-periodic pattern with a period of about 1.7 μm is observed on the wire (Figure 7iii). The modulated near-field distribution pattern shows the phenomenon of spatial beating, caused by the superposition of excited plasmon modes. If the polarization of the incident light is rotated, as shown in Figure 7iv, the plasmon-induced near-field distribution pattern is changed, with the local field distributed on the two sides of the nanowire. The near-field distribution pattern can be controlled by the incident polarization. When the polarization is rotated to the direction shown in Figure 7vi, the near-field pattern becomes opposite to that shown in Figure 7iv. For incident polarization perpendicular to the nanowire, the intensity of launched plasmons in the wire becomes weak (Figure 7v). The different local field distribution pattern under different polarizations is caused by the different relative intensities of the plasmon modes excited in the wire.

For the system in Figure 7, the nanowire is placed on a glass substrate with air surrounding the top of the wire, making the dielectric environment quite asymmetric. If the nanowire is located in a uniform dielectric medium, the plasmon properties are different. Figure 8A and 8B show the simulation results for a silver nanowire in a uniform medium with a refractive index of 1.5, which can be realized in experiments by depositing the nanowire on a glass substrate and coating with index-matching oil. For an incident polarization with an angle of 45° relative to the wire axis (Figure 8A), the three modes (m=0, 1, -1) will be excited simultaneously. The surface charge density on the wire is distributed in a helical way [44]. From time-averaged power flow in the plane perpendicular to the nanowire at different positions along the wire, the rotation of the energy flow around the nanowire is clearly observed (Figure 8B). The distance along the nanowire for the energy flow to encircle the wire is the period of the helix. For a nanowire of 60 nm radius shown in Figure 8A, the helix period is 1.83 μm. The period of the plasmon helix is proportional to the inverse of the difference between the propagation constants of the m=0 mode and m=1 (or m=-1) mode. With an increase of the nanowire thickness, the helix period increases (Figure 8C).

The helically propagating plasmons may be left-handed or right-handed depending on the phase difference between the m=1 and m=-1 modes, which can be controlled by tuning the incident polarization angle. Figure 8D shows the experimentally observed chiral SPPs imaged by QD fluorescence. The chirality disappears when the incident polarization is parallel or perpendicular to the nanowire. The near-field distributions in Figure 7iv and 7vi can be regarded as distorted chiral surface plasmons.

2.5. Electrical generation and detection of SPPs

The generation and detection of surface plasmons are usually based on large optical sources and detectors. To facilitate

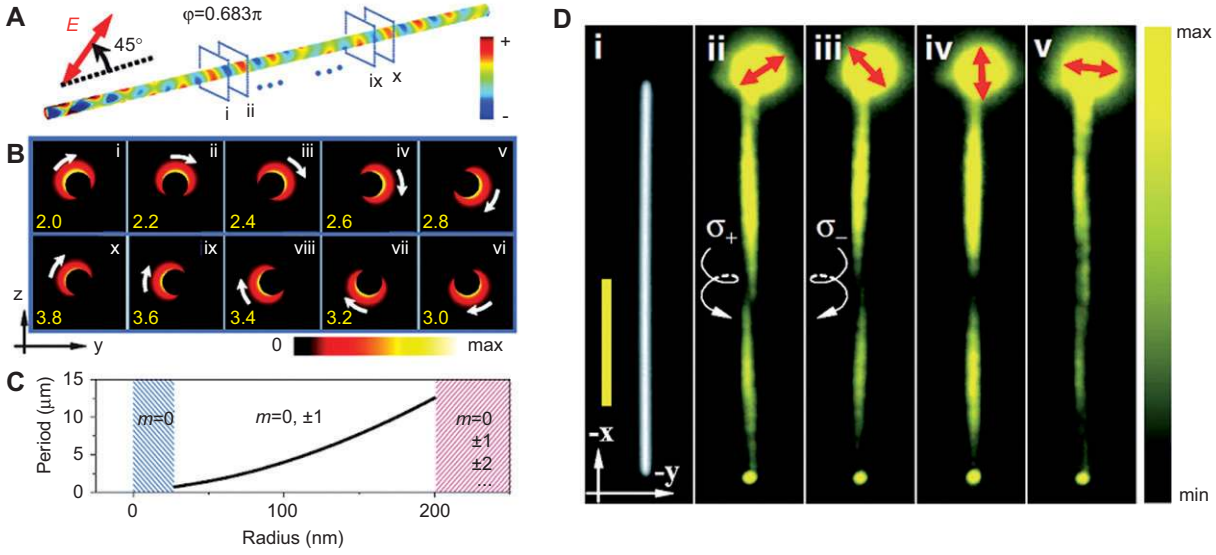

Figure 8 Chiral SPPs (A) Surface charge density plot on a Ag nanowire. The maximum value of the surface charge was truncated at the incident end to better show the plasmon modes on the wire. The length of the simulated nanowire (R=60 nm) is L=5.0 μm and the incident polarization angle is θ=45° in (A) and (B). (B) Time-averaged power flow in the yz plane at different positions along the nanowire, where x=2.0–3.8 μm (i–x) in steps of 0.2 μm, indicated by the blue frames in (A). The white arrows highlight the rotation of electromagnetic energy as a function of position along the nanowire, showing right-handed chiral SPPs. (C) Periods of the plasmon helix, Λ, as a function of nanowire radius. The blue region denotes the single mode-dominant regime and the magenta region denotes the multimode regime. (D) (i) Optical image of a Ag nanowire. The scale bar is 5 μm. (ii, iii) Quantum dot fluorescence images of right-handed (ii) and left-handed (iii) SPPs, respectively. The white helical arrows highlight the handedness of the plasmon helix. The wavelength of the laser light for excitation is 632.8 nm [44].

the integration of plasmonic components, the development of compact plasmon sources and detectors is an urgent task. Falk et al. demonstrated an electrical detection method for propagating plasmons in metal nanowires by using a Ge nanowire field-effect transistor (Figure 9A) [78]. The silver nanowire is placed across the Ge nanowire. When surface plasmons propagate on the silver wire, electron-hole pairs will be generated in the Ge wire and an electrical current will be formed in the Ge nanowire device. The surface plasmons are detected by measuring the electrical signal. The current map in Figure 9B shows the current through the Ge nanowire when the excitation laser was placed at different positions. As well as direct illumination on the Ge wire, a strong current appears when the laser light illuminates the silver nanowire terminals. This is because surface plasmons can only be excited at the two ends of the silver wire. Electrical detection of gap plasmons has also been demonstrated by Neutens et al. by using an integrated metal-semiconductor-metal photodetector [79]. By using the gating effect of surface plasmons on metal quantum point contacts, surface plasmons were also detected electrically [80].

Electrical excitation of surface plasmons in gold nanowires has recently been demonstrated by Bharadwaj et al. [81]. They used a scanning tunneling microscope (STM) with a gold tip to approach a gold nanowire. By employing inelastic electron tunneling between the tip and the wire, localized gap plasmons in the tip-wire junction are excited. The gap plasmons then couple to propagating plasmons in the gold nanowire, which are detected by the scattered photons at the output end of the wire (Figure 9C and 9D). Based on light-emitting diodes and silicon nanocrystals, electrically switchable surface plasmon sources were demonstrated [82–84]. A quantum cascade laser has also been employed for electrical generation of surface plasmons [85].

2.6. Nanowire-emitter coupling

The emitters will couple to plasmonic nanowires if they are in close proximity. The coupling between surface plasmons and the emitters has fundamental importance for tailoring light-matter interaction, and for the development of SPP-based nanophotonic devices. For example, the integration of passive metallic nanowire waveguides and active semiconductor materials can be expected for functional elements with outstanding performances. Figure 10 summarizes the processes in the nanowire-emitter system. Surface plasmons excited by

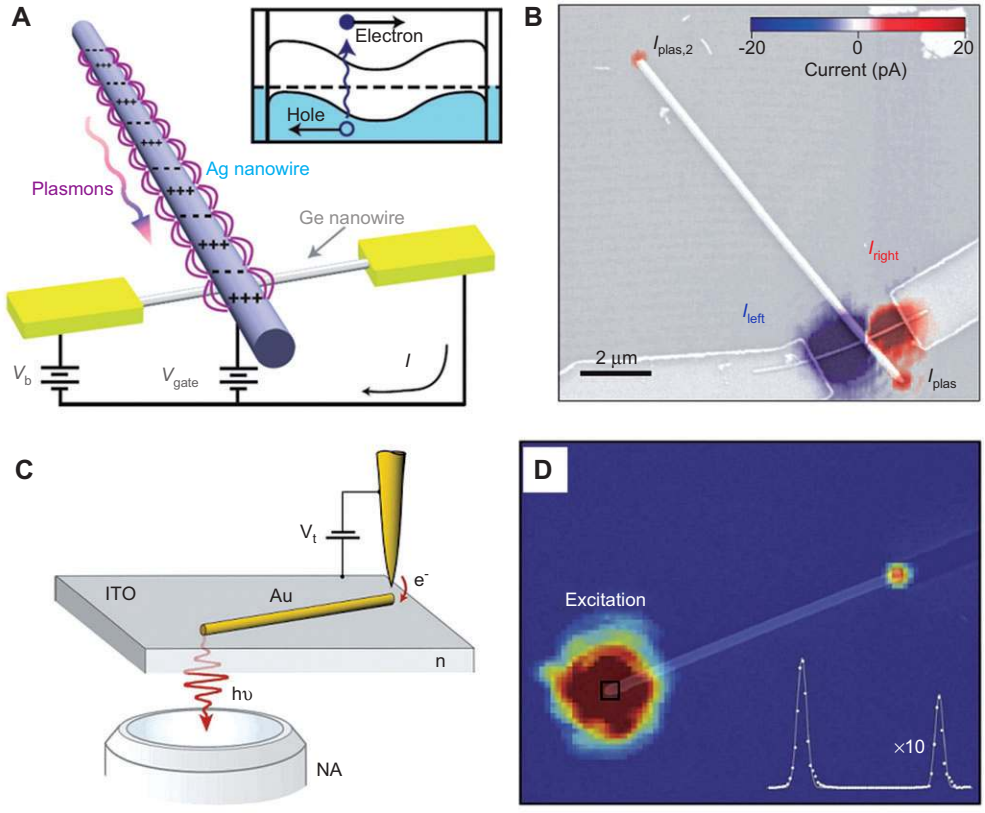

Figure 9 (A) Schematic diagram of the electrical plasmon detector operation. Inset: Electron–hole pair generation and separation in the Ge nanowire detector. (B) Scanning electron micrograph of the device, overlaid with the current through the Ge nanowire as a function of excitation laser position. Excitation laser power P=2.0 µW, wavelength λ_{ex}=532 nm, V_b=0, V_{gate}=0. (C) Illustration of the experiment for electrical plasmon generation. Inelastic electron tunneling between a gold tip and a single-crystal gold nanorod gives rise to surface plasmon excitation. (D) Photon emission map superimposed on an SEM image. SPPs excited at one end of the wire propagate to the other end [78, 81].

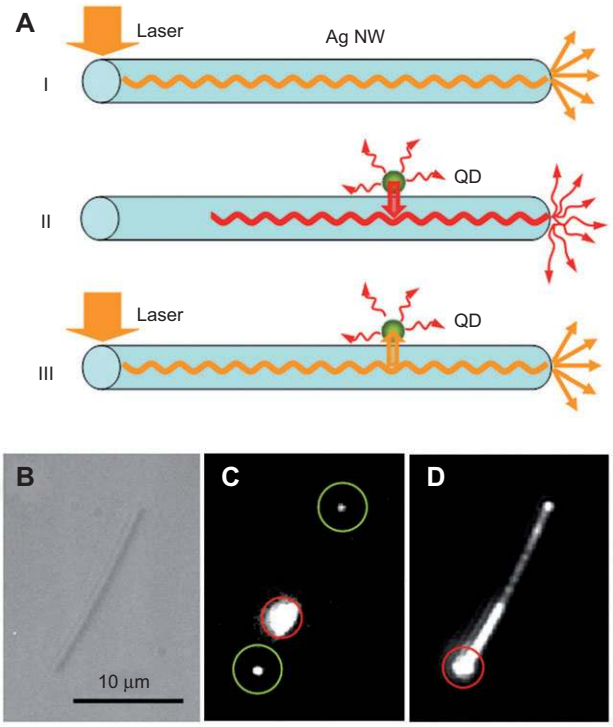

Figure 10 (A) Schematic illustration of the processes in a silver nanowire (Ag NW)-quantum dot (QD) system. (B) Optical image of a silver nanowire. (C, D) QD fluorescence images for laser excitation at the midsection of the wire (B) and bottom end of the wire (D). The positions of excitation are marked by red circles [86].

the incident light propagate along the wire and partly couple out at the output end of the wire (Process I). The decay of an excited emitter (QD) may also generate propagating plasmons in the nanowire (Process II). Plasmons propagating in the nanowire can excite a nearby emitter, if the plasmon energy is within the absorption band of the emitter (Process III), which is the basis for the fluorescence imaging of local plasmon field distributions. The coupling efficiency between and nanowire plamons and the emitters depends strongly on the separation between the wire and emitter. Other parameters, such as the diameter of the nanowire, the plasmon wavelength, the absorption and emission band of the emitter, also influence the coupling efficiency.

The generation of single plasmons by an excited quantum dot was demonstrated by Akimov et al. [87]. Single surface plasmons excited by single nitrogen-vacancy (NV) defects in diamond nanocrystals was demonstrated by Kolesov et al., and they showed that single plasmons behave like single photons, exhibiting wave-particle duality [88]. Theoretical work has been performed to study the coupling between quantum emitters and metal nanowires, and the applications of plasmonic waveguides in quantum technology [89–96]. Manipulation based on an atomic force microscope has been utilized to control the coupling between nanowires and emitters [97, 98]. The propagating plasmons have also been used to remotely excite the Raman scattering of molecules, located away from the excitation spot [99, 100].

3. Optical signal control and processing in nanowire networks

3.1. SPP routing

Plasmons propagating in a nanowire can be converted to photons by scattering at the nanowire end and other structural anomalies, such as the nanoparticles adhering to the wire. Figure 11A shows a structure composed of a silver nanowire and silver nanoparticle. The intensity of the scattered light at the particle position depends strongly on the polarization of the excitation light (Figure 11Aiii and 11Av). The mechanism of the polarization-dependent scattering intensity is revealed by using quantum dot fluorescence imaging. Figure 11Aiv shows the near-field distribution for the polarization shown in Figure 11Aiii. As can be seen, the nanoparticle-nanowire junction overlaps with one of the antinodes of the near-field distribution pattern. The strong near-field intensity at the junction results in stronger scattering. For the polarization shown in Figure 11Av, the near-field intensity at the junction is very low (Figure 11Avi). There is almost no light scattered by the particle. Therefore, the polarization-dependent near-field distribution can be used to control the energy transmitted to the connected structures.

If the nanoparticle is replaced by a nanowire, a branched structure is obtained. The plasmons excited in the primary wire have two transmission routes. For the structure shown in Figure 11B, laser light of 633 nm and 785 nm wavelengths were used for plasmon excitation. The output intensity at both terminals 2 and 3 depend strongly on the incident polarization. The energy can be routed in a controlled manner to terminal 2 or terminal 3 by manipulating the polarization of the excitation light. However, the polarization dependence for 633 nm excitation and 785 nm excitation is quite different (Figure 11C). For a fixed incident polarization of 40° as shown in Figure 11D, both laser light of 633 nm and 785 nm are focused onto terminal 1 simultaneously to launch propagating plasmons. The spectra obtained at terminal 2 and terminal 3 show that most of the 633 nm light travels to terminal 2, while most of the 785 nm light is transmitted to terminal 3. This means the branched nanowire structure can serve as a de-multiplexer to direct signals of different frequencies to different routes. The modulated near-field distribution pattern on the nanowire is caused by the superposition of different plasmons modes. For different excitation wavelengths, the near-field distribution patterns are different, which enables a separation of light signals of different wavelengths.

3.2. SPP-Interference-based logic gates and half adder

In a branched nanowire structure composed of a main wire and a branch wire, the branch nanowire can serve as an input to launch a second plasmon beam into the main nanowire. The two plasmon beams interfere in the main wire and modulate the near field distribution. As the phase difference between two incident laser beams is varied, the near-field distribution on the main wire is changed, and thus, the output intensity at

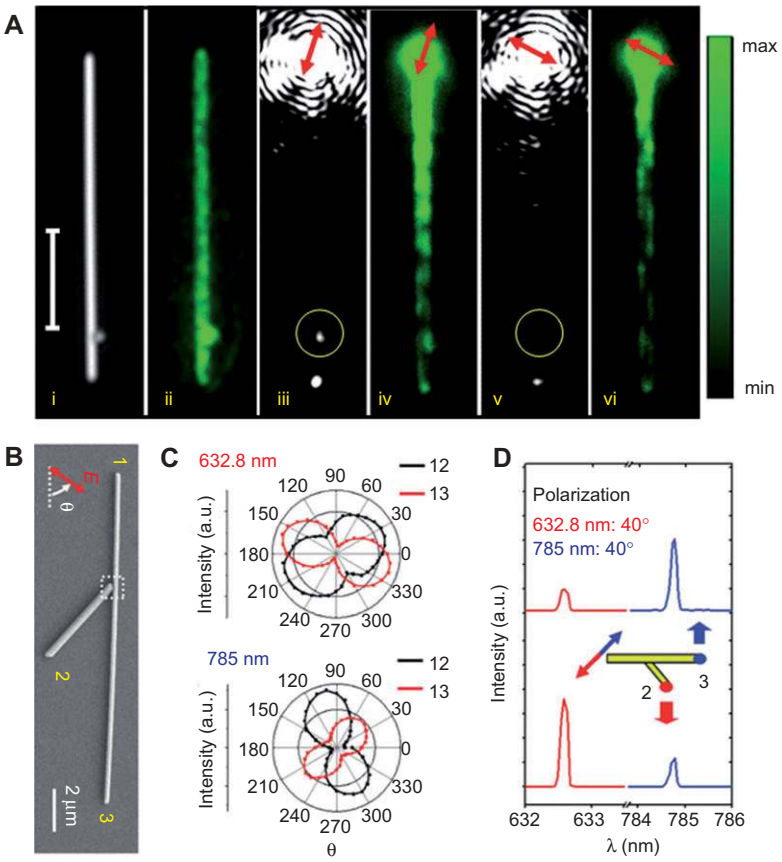

Figure 11 (A) QD emission images of plasmons launched by 633 nm laser excitation at one end of a Ag nanowire. Changing the polarization angle at the input end controls the emission from an adjacent Ag nanoparticle at the opposite end of the wire. (i) Optical image of a nanowire-nanoparticle system. (ii) QD emission image with wide field excitation. (iii, v) Scattering images. (iv, vi) QD emission images corresponding to (iii) and (v), respectively. The scale bar is 5 μm. The red arrows indicate the laser polarization. (B) The SEM image of a branched silver nanowire structure. θ is the angle of the incident polarization. (C) Emission intensity from nanowire end 2 (black) and 3 (red) as a function of incident polarization angle for 633 nm and 785 nm wavelength excitation. (D) The spectra collected from wire end 2 (lower curves) and 3 (upper curves). The polarization angle of the incident light is 40° [77, 101].

the main wire terminal oscillates [102]. If another branch is connected to the main wire for signal routing (Figure 12Ai), as the phase difference between two laser beams is tuned, the output intensity at both output terminals varies. For certain phases, the signal can be routed selectively to output O1 or output O2 (Figure 12Aii and 12Aiii). The near-field distributions revealed by QD imaging show that the near-field intensities at the two output arms change in an alternate manner. A strong near-field intensity results in a strong output intensity. The switching of the signal between the two arms is determined by the near-field intensity at the junction where the output branch is connected to the main wire. When the near-field intensity in the junction (encircled by a dashed yellow rectangle) is weak, the energy propagates to terminal O1 (Figure 12Aiv). When the intensity in the junction is strong, most of the energy is switched to the branch wire and guided to terminal O2 (Figure 12Av). Besides the polarization, the SPP interference as determined by the phase provides another way to control the signal routing in the nanowire network. The combination of polarization and phase can achieve additional control of the signal distribution that cannot be realized by controlling only polarization or phase.

The strong and weak output intensity can be assigned as "ON" and "OFF" states. By defining certain intensity values as thresholds for "1" and "0", the nanowire structures can realize some logical operations. Considering I1 and I2 as the inputs and O2 as the output, the structure shown in Figure 12A can serve as an AND gate. A complete set of logic operations can be realized in nanowire-based structures. The structure in Figure 12A can also be regarded as a binary half adder, in which I1 and I2 are inputs for two one-bit binary numbers, O1 is for the sum and O2 is for the value carried on to the next addition.

To realize more complex functions, the cascade of these basic logic gates is needed. It is demonstrated that a NOR gate, one of the universal logic gates, can be cascaded by an OR gate and a NOT gate. The working principle and the designed structure are shown in Figure 12B. The left part of the long wire and the left branch wire perform the OR operation, while the right part of the long wire and the right branch

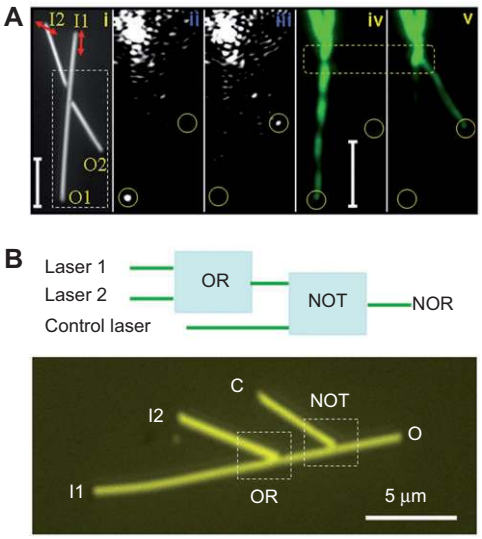

Figure 12 (A) Modulation and routing of light in a two input – two output nanowire network. (i) Optical image of the network. (ii, iii) Scattering images for two beam interference resulting in output at O1 terminal and O2 terminal, respectively. (iv, v) QD emission images corresponding to (ii) and (iii). Al_2O_3 thickness is 50 nm. Scale bar is 5 μm. Red arrows in (i) show the polarization of the two laser beams, and the white dashed rectangle in (i) marks the area displayed in (ii–v). (B) Schematic illustration of a NOR logic gate, built by cascaded OR and NOT gates (top) and optical image of the designed Ag nanowire structure [77, 103].

wire perform the NOT operation. The operation result of the OR gate is inverted by the NOT gate, and a NOR gate is realized. The mechanism of this device was revealed by QD fluorescence imaging. For the inputs at either or both I1 and I2, the control branch junction needs to be overlapped with one of the antinodes in the near-field distribution pattern, i.e.,

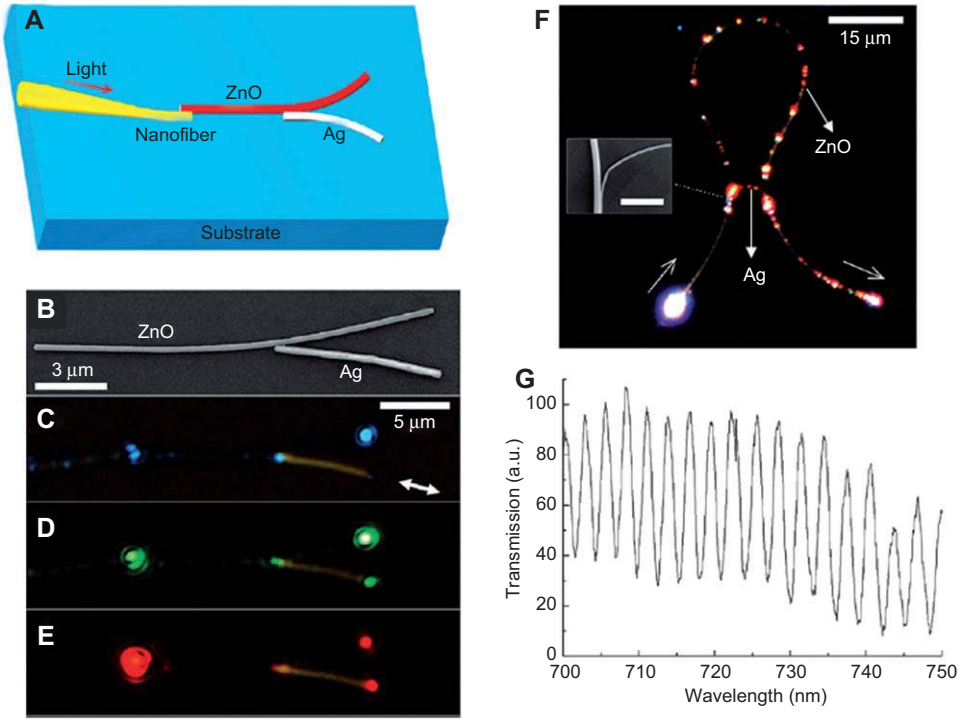

Figure 13 (A) Schematic of a hybrid coupler fabricated from coupled Ag and ZnO nanowires. (B) SEM image of a hybrid coupler assembled from a 270 nm diameter ZnO nanowire and a 240 nm diameter Ag nanowire. (C–E) Optical micrographs of the hybrid coupler taken with the polarization parallel to the Ag nanowire when monochromatic lasers of wavelength 488, 532 and 650 nm were used as light sources. (F) Optical microscope image of a hybrid Mach-Zehnder interferometer (MZI) assembled using a 330 nm diameter ZnO nanowire and a 120 nm diameter Ag nanowire on a MgF_2 crystal, with a white light excitation source. Inset: a SEM image of the coupling area. Scale bar is 2 μm. (G) Transmission spectrum measured with a white light source [104].

the near-field intensity at that junction is locally strong. The strong field intensity at the junction guarantees that the control signal can strongly interfere with the signal coming from the OR gate and invert the OR operation result.

The optical signal controlling and processing discussed here, are all based on control of the near-field distributions of plasmons propagating in simple nanowire networks. The engineering to the near-field distribution should be regarded as a rule for designing functional nanowire-based devices and networks. The QD fluorescence imaging method developed for the nanowire systems is a powerful tool to characterize the plasmon field distributions, and can potentially be extended to studies in other systems.

4. Hybrid structures and devices

Due to the high loss of plasmons propagating in metal nanowires, the propagation distance is limited. The incorporation of photonic nanowires with metal nanowires may help to solve this problem. Both experimental and theoretical efforts have been devoted to coupled photonic and plasmonic waveguides. Guo et al. demonstrated the coupling of Ag nanowire and ZnO nanowire [104]. Figure 13A shows a hybrid coupler of ZnO and Ag nanowires. Light was coupled into the ZnO nanowire through a tapered optical fiber. Part of the light can be directed to the Ag nanowire by near-field coupling (Figure 13C–E). If propagating plasmons in Ag nanowires are excited first, the plasmons can also be converted to guided photonic modes in the ZnO wire. For the structure in Figure 13B, the coupling efficiency from the ZnO nanowire to the Ag nanowire at wavelength of 650 nm is about 82% after considering the guiding loss of plasmons in Ag nanowire. By coupling both ends of a silver nanowire to a ZnO nanowire, a hybrid Mach-Zehnder interferometer was made (Figure 13F). When white light was put in from one end of the ZnO nanowire, the output light from the other end of the ZnO wire shows strong modulations in the transmission spectrum (Figure 13G). The coupling of light from polymer waveguide and optical fiber into silver nanowires was studied by Pyayt et al. and Dong et al., respectively [105, 106]. Coupling between Ag nanowire and SnO_2 nanoribbon was investigated by Yan et al. [107]. Chen et al. investigated the coupling between a metal nanowire and a dielectric fiber theoretically. They showed that the plasmon-photon conversion efficiency can be larger than 95% in the visible and near-infrared [108].

Besides the hybrid waveguides, many components developed for nanophotonic circuits are also based on hybrid structures of metal and other materials. Pala et al. demonstrate an all-optical switch that combines the properties of plasmonic nanostructures and small molecules [109]. Research groups have explored the electro-optical modulation of optical signals in hybrid structures [110–112]. Magneto-plasmonic interferometry in hybrid metal-ferromagnet structures was demonstrated by Temnov et al. [113]. Hybrid structures have been employed to make plasmonic lasers and light sources [114–117]. More references about the plasmon-involved amplifiers and light sources can be found in a recent review paper by Berini et al. [118]. The hybridization of different materials can produce functionalities and performances not achievable by a single material only. The development of these hybrid devices will promote the building of nanophotonic circuits for on-chip integration applications.

5. Conclusions and Outlook

Metal nanowires are promising as waveguides to transport light signals in nanophotonic circuits. The properties of plasmons propagating in the nanowires, such as emission direction and polarization, group velocity, loss and near-field distribution, have been revealed. Based on our understanding of the nanowire plasmons, devices for specific signal control and processing can be designed. The coupling between metal nanowires and emitters or other materials provides more possibilities to realize functional components for the construction of nanophotonic circuits with unprecedented performances.

In spite of the advancement in the research of functional elements, there is still a long way to make functional nanophotonic circuits for real applications. The optimization of device functionalities and the development of new design schemes need to be conducted. To build a functional plasmon-based circuit, the integration of different components is an inevitable issue and a challenging task. The hybridization of plasmonic structures with materials with outstanding properties, such as opto-electric, electro-optical, and nonlinear materials, will advance the development of nanophotonic devices. The interfacing of nanophotonic circuits with electronic devices and the compatibility of fabrication technologies are also important issues. Nanophotonic circuits built by plasmonic waveguides can potentially be used for quantum information processing in place of the larger size photonic circuits [119, 120].

Acknowledgements

This work was supported by MOST Grants (2009CB930700), NSFC Grants (Nos.10625418, 10874233, 11004237 and 11134013), and "Knowledge Innovation Project" (KJCX2-EW-W04) of CAS.

References

[1] Barnes WL, Dereux A, Ebbesen TW. Surface plasmon subwavelength optics. Nature 2003;424:824–30.
[2] Schuller JA, Barnard ES, Cai WS, Jun YC, White JS, Brongersma ML. Plasmonics for extreme light concentration and manipulation. Nat Mater 2010;9:193–204.
[3] Kelly KL, Coronado E, Zhao LL, Schatz GC. The optical properties of metal nanoparticles: the influence of size, shape, and dielectric environment. J Phys Chem B 2003;107:668–77.
[4] Campbell CT, Kim G. SPR microscopy and its applications to high-throughput analyses of biomolecular binding events and their kinetics. Biomaterials 2007;28:2380–92.
[5] Mayer KM, Hafner JH. Localized surface plasmon resonance sensors. Chem Rev 2011;111:3828–57.

[6] Xu HX, Bjerneld EJ, Kall M, Borjesson L. Spectroscopy of single hemoglobin molecules by surface enhanced Raman scattering. Phys Rev Lett 1999;83:4357–60.
[7] Xu HX, Aizpurua J, Kall M, Apell P. Electromagnetic contributions to single-molecule sensitivity in surface-enhanced Raman scattering. Phys Rev E 2000;62:4318–24.
[8] Moskovits M. Surface-enhanced Raman spectroscopy: a brief retrospective. J Raman Spec 2005;36:485–96.
[9] Xu HX, Kall M. Surface-plasmon-enhanced optical forces in silver nanoaggregates. Phys Rev Lett 2002;89:246802.
[10] Juan ML, Righini M, Quidant R. Plasmon nano-optical tweezers. Nat Photon 2011;5:349–56.
[11] Tong LM, Miljkovic VD, Kall M. Alignment, rotation, and spinning of single plasmonic nanoparticles and nanowires using polarization dependent optical forces. Nano Lett 2010;10:268–73.
[12] Muhlschlegel P, Eisler HJ, Martin OJF, Hecht B, Pohl DW. Resonant optical antennas. Science 2005;308:1607–9.
[13] Kim S, Jin JH, Kim YJ, Park IY, Kim Y, Kim SW. High-harmonic generation by resonant plasmon field enhancement. Nature 2008;453:757–60.
[14] Shegai T, Li ZP, Dadosh T, Zhang ZY, Xu HX, Haran G. Managing light polarization via plasmon-molecule interactions within an asymmetric metal nanoparticle trimer. Proc Natl Acad Sci USA 2008;105:16448–53.
[15] Novotny L, van Hulst N. Antennas for light. Nat Photon 2011;5:83–90.
[16] Lal S, Clare SE, Halas NJ. Nanoshell-enabled photothermal cancer therapy: impending clinical impact. Accounts Chem Res 2008;41:1842–51.
[17] Atwater HA, Polman A. Plasmonics for improved photovoltaic devices. Nat Mater 2010;9:205–13.
[18] Linic S, Christopher P, Ingram DB. Plasmonic-metal nanostructures for efficient conversion of solar to chemical energy. Nat Mater 2011;10:911–21.
[19] Weeber JC, Krenn JR, Dereux A, Lamprecht B, Lacroute Y, Goudonnet JP. Near-field observation of surface plasmon polariton propagation on thin metal stripes. Phys Rev B 2001;64:045411.
[20] Krenn JR, Lamprecht B, Ditlbacher H, Schider G, Salerno M, Leitner A, Aussenegg FR. Non–diffraction-limited light transport by gold nanowires. Europhys Lett 2002;60:663–9.
[21] Zia R, Schuller JA, Brongersma ML. Near-field characterization of guided polariton propagation and cutoff in surface plasmon waveguides. Phys Rev B 2006;74:165415.
[22] Pile DFP, Ogawa T, Gramotnev DK, Okamoto T, Haraguchi M, Fukui M, Matsuo S. Theoretical and experimental investigation of strongly localized plasmons on triangular metal wedges for subwavelength waveguiding. Appl Phys Lett 2005;87:061106.
[23] Pile DFP, Gramotnev DK. Channel plasmon-polariton in a triangular groove on a metal surface. Opt Lett 2004;29:1069–71.
[24] Bozhevolnyi SI, Volkov VS, Devaux E, Laluet JY, Ebbesen TW. Channel plasmon subwavelength waveguide components including interferometers and ring resonators. Nature 2006;440:508–11.
[25] Pile DFP, Ogawa T, Gramotnev DK, Matsuzaki Y, Vernon KC, Yamaguchi K, Okamoto T, Haraguchi M, Fukui M. Two-dimensionally localized modes of a nanoscale gap plasmon waveguide. Appl Phys Lett 2005;87:261114.
[26] Veronis G, Fan SH. Guided subwavelength plasmonic mode supported by a slot in a thin metal film. Opt Lett 2005;30:3359–61.
[27] Dionne JA, Sweatlock LA, Atwater HA, Polman A. Plasmon slot waveguides: towards chip-scale propagation with subwavelength-scale localization. Phys Rev B 2006;73:035407.
[28] Steinberger B, Hohenau A, Ditlbacher H, Stepanov AL, Drezet A, Aussenegg FR, Leitner A, Krenn JR. Dielectric stripes on gold as surface plasmon waveguides. Appl Phys Lett 2006;88:094104.
[29] Papaioannou S, Vyrsokinos K, Tsilipakos O, Pitilakis A, Hassan K, Weeber JC, Markey L, Dereux A, Bozhevolnyi SI, Miliou A, Kriezis EE, Pleros N. A 320 Gb/s-throughput capable 2×2 silicon-plasmonic router architecture for optical interconnects. J Lightwave Technol 2011;29:3185–95.
[30] Ditlbacher H, Hohenau A, Wagner D, Kreibig U, Rogers M, Hofer F, Aussenegg FR, Krenn JR. Silver nanowires as surface plasmon resonators. Phys Rev Lett 2005;95:257403.
[31] Sanders AW, Routenberg DA, Wiley BJ, Xia YN, Dufresne ER, Reed MA. Observation of plasmon propagation, redirection, and fan-out in silver nanowires. Nano Lett 2006;6:1822–6.
[32] Knight MW, Grady NK, Bardhan R, Hao F, Nordlander P, Halas NJ. Nanoparticle-mediated coupling of light into a nanowire. Nano Lett 2007;7:2346–50.
[33] Wang WH, Yang Q, Fan FR, Xu HX, Wang ZL. Light propagation in curved silver nanowire plasmonic waveguides. Nano Lett 2011;11:1603–8.
[34] Fang ZY, Fan LR, Lin CF, Zhang D, Meixner AJ, Zhu X. Plasmonic coupling of bow tie antennas with Ag nanowire. Nano Lett 2011;11:1676–80.
[35] Kinzel EC, Xu XF. High efficiency excitation of plasmonic waveguides with vertically integrated resonant bowtie apertures. Opt Express 2009;17:8036–45.
[36] Normatov A, Spektor B, Leviatan Y, Shamir J. Absorption enhancement by matching the cross-section of plasmonic nanowires to the field structure of tightly focused beams. Opt Express 2011;19:8506–13.
[37] Hohenau A, Krenn JR, Drezet A, Mollet O, Huant S, Genet C, Stein B, Ebbesen TW. Surface plasmon leakage radiation microscopy at the diffraction limit. Opt Express 2011;19:25749–62.
[38] Shegai T, Miljkovic VD, Bao K, Xu HX, Nordlander P, Johansson P, Kall M. Unidirectional broadband light emission from supported plasmonic nanowires. Nano Lett 2011;11:706–11.
[39] Lieb MA, Zavislan JM, Novotny L. Single-molecule orientations determined by direct emission pattern imaging. J Opt Soc Am B 2004;21:1210–5.
[40] Song MX, Bouhelier A, Bramant P, Sharma J, Dujardin E, Zhang DG, Colas-des-Francs G. Imaging symmetry-selected corner plasmon modes in penta-twinned crystalline Ag nanowires. Acs Nano 2011;5:5874–80.
[41] Shegai T, Chen S, Miljkovic VD, Zengin G, Johansson P, Kall M. A bimetallic nanoantenna for directional colour routing. Nat Commun 2011;2:481.
[42] Grandidier J, Francs GC, Massenot S, Bouhelier A, Markey L, Weeber JC, Dereux A. Leakage radiation microscopy of surface plasmon coupled emission: investigation of gain assisted propagation in an integrated plasmonic waveguide. J Microsc 2010;239:167–72.
[43] Li ZP, Bao K, Fang YR, Huang YZ, Nordlander P, Xu HX. Correlation between incident and emission polarization in nanowire surface plasmon waveguides. Nano Lett 2010;10:1831–5.
[44] Zhang SP, Wei H, Bao K, Hakanson U, Halas NJ, Nordlander P, Xu HX. Chiral surface plasmon polaritons on metallic nanowires. Phys Rev Lett 2011;107:096801.

[45] Allione M, Temnov VV, Fedutik Y, Woggon U, Artemyev MV. Surface plasmon mediated interference phenomena in low-Q silver nanowire cavities. Nano Lett 2008;8:31–5.
[46] Kusar P, Gruber C, Hohenau A, Krenn JR. Measurement and reduction of damping in plasmonic nanowires. Nano Lett 2012;12:661–5.
[47] Rewitz C, Keitzl T, Tuchscherer P, Huang J, Geisler P, Razinskas G, Hecht B, Brixner T. Ultrafast plasmon propagation in nanowires characterized by far-field spectral interferometry. Nano Lett 2012;12:45–9.
[48] Ma YG, Li XY, Yu HK, Tong LM, Gu Y, Gong QH. Direct measurement of propagation losses in silver nanowires. Opt Lett 2010;35:1160–2.
[49] Li Q, Wang SS, Chen YT, Yan M, Tong LM, Qiu M. Experimental demonstration of plasmon propagation, coupling, and splitting in silver nanowire at 1550-nm wavelength. IEEE J Sel Top in Quantum Electron 2011;17:1107–11.
[50] Shegai T, Huang YZ, Xu HX, Kall M. Coloring fluorescence emission with silver nanowires. Appl Phys Lett 2010;96:103114.
[51] Solis D, Chang WS, Khanal BP, Bao K, Nordlander P, Zubarev ER, Link S. Bleach-imaged plasmon propagation (BlIPP) in single gold nanowires. Nano Lett 2010;10:3482–5.
[52] Li ZP, Bao K, Fang YR, Guan ZQ, Halas NJ, Nordlander P, Xu HX. Effect of aproximal substrate on plasmon propagation in silver nanowires. Phys Rev B 2010;82:241402.
[53] Manjavacas A, de Abajo FJG. Robust plasmon waveguides in strongly interacting nanowire arrays. Nano Lett 2009;9:1285–9.
[54] Oulton RF, Sorger VJ, Genov DA, Pile DFP, Zhang X. A hybrid plasmonic waveguide for subwavelength confinement and long-range propagation. Nat Photon 2008;2:496–500.
[55] Namassivayane K, Tanvir H, Quadir A, Rahman BMA, Grattan KTV. Study of modal properties in gold nanowire with ZnO cladding by using the finite element method. Appl Optics 2011;50:E177–83.
[56] Szafranek D, Leviatan Y. A source-model technique for analysis of wave guiding along chains of metallic nanowires in layered media. Opt Express 2011;19:25397–411.
[57] Krasavin AV, Zayats AV. Guiding light at the nanoscale: numerical optimization of ultrasubwavelength metallic wire plasmonic waveguides. Opt Lett 2011;36:3127–9.
[58] Kou Y, Ye FW, Chen XF. Low-loss hybrid plasmonic waveguide for compact and high-efficient photonic integration. Opt Express 2011;19:11746–52.
[59] Cao L, Nome RA, Montgomery JM, Gray SK, Scherer NF. Controlling plasmonic wave packets in silver nanowires. Nano Lett 2010;10:3389–94.
[60] Zhang ZX, Hu ML, Chan KT, Wang CY. Plasmonic waveguiding in a hexagonally ordered metal wire array. Opt Lett 2010;35:3901–3.
[61] Lei DY, Aubry A, Maier SA, Pendry JB. Broadband nanofocusing of light using kissing nanowires. New J Phys 2010;12:093030.
[62] Bergman DJ, Stockman MI. Surface plasmon amplification by stimulated emission of radiation: quantum generation of coherent surface plasmons in nanosystems. Phys Rev Lett 2003;90:027402.
[63] Seidel J, Grafstrom S, Eng L. Stimulated emission of surface plasmons at the interface between a silver film and an optically pumped dye solution. Phys Rev Lett 2005;94:177401.
[64] Noginov MA, Zhu G, Mayy M, Ritzo BA, Noginova N, Podolskiy VA. Stimulated emission of surface plasmon polaritons. Phys Rev Lett 2008;101:226806.
[65] Grandidier J, Francs GCD, Massenot S, Bouhelier A, Markey L, Weeber JC, Finot C, Dereux A. Gain-assisted propagation in a plasmonic waveguide at telecom wavelength. Nano Lett 2009;9:2935–9.
[66] De Leon I, Berini P. Amplification of long-range surface plasmons by a dipolar gain medium. Nat Photon 2010;4:382–7.
[67] Gather MC, Meerholz K, Danz N, Leosson K. Net optical gain in a plasmonic waveguide embedded in a fluorescent polymer. Nat Photon 2010;4:457–61.
[68] Bolger PM, Dickson W, Krasavin AV, Liebscher L, Hickey SG, Skryabin DV, Zayats AV. Amplified spontaneous emission of surface plasmon polaritons and limitations on the increase of their propagation length. Opt Lett 2010;35:1197–9.
[69] Li DB, Ning CZ. Giant modal gain, amplified surface plasmon-polariton propagation, and slowing down of energy velocity in a metal-semiconductor-metal structure. Phys Rev B 2009;80:153304.
[70] des Francs GC, Bramant P, Grandidier J, Bouhelier A, Weeber JC, Dereux A. Optical gain, spontaneous and stimulated emission of surface plasmon polaritons in confined plasmonic waveguide. Opt Express 2010;18:16327–34.
[71] Saleh AAE, Dionne JA. Waveguides with a silver lining: low threshold gain and giant modal gain in active cylindrical and coaxial plasmonic devices. Phys Rev B 2012;85:045407.
[72] Handapangoda D, Rukhlenko ID, Premaratne M, Jagadish C. Optimization of gain-assisted waveguiding in metal-dielectric nanowires. Opt Lett 2010;35:4190–2.
[73] Khurgin JB, Sun G. Practicality of compensating the loss in the plasmonic waveguides using semiconductor gain medium. Appl Phys Lett 2012;100:011105.
[74] Li YC, Zhang H, Zhu N, Mei T, Zhang DH, Teng JH. Short-range surface plasmon propagation supported by stimulated amplification using electrical injection. Opt Express 2011;19:22107–12.
[75] Sorger VJ, Ye Z, Oulton RF, Wang Y, Bartal G, Yin X, Zhang X. Experimental demonstration of low-loss optical waveguiding at deep sub-wavelength scales. Nat Commun 2011;2:331.
[76] Ditlbacher H, Krenn JR, Felidj N, Lamprecht B, Schider G, Salerno M, Leitner A, Aussenegg FR. Fluorescence imaging of surface plasmon fields. Appl Phys Lett 2002;80:404–6.
[77] Wei H, Li ZP, Tian XR, Wang ZX, Cong FZ, Liu N, Zhang SP, Nordlander P, Halas NJ, Xu HX. Quantum dot-based local field imaging reveals plasmon-based interferometric logic in silver. Nano Lett 2011;11:471–5.
[78] Falk AL, Koppens FHL, Yu CL, Kang K, Snapp ND, Akimov AV, Jo MH, Lukin MD, Park H. Near-field electrical detection of optical plasmons and single-plasmon sources. Nat Phys 2009;5:475–9.
[79] Neutens P, Van Dorpe P, De Vlaminck I, Lagae L, Borghs G. Electrical detection of confined gap plasmons in metal-insulator-metal waveguides. Nat Photon 2009;3:283–6.
[80] Ittah N, Selzer Y. Electrical detection of surface plasmon polaritons by 1G0 gold quantum point contacts. Nano Lett 2011;11:529–34.
[81] Bharadwaj P, Bouhelier A, Novotny L. Electrical excitation of surface plasmons. Phys Rev Lett 2011;106:226802.
[82] Koller DM, Hohenau A, Ditlbacher H, Galler N, Reil F, Aussenegg FR, Leitner A, List EJW, Krenn JR. Organic plasmon-emitting diode. Nat Photon 2008;2:684–7.
[83] Neutens P, Lagae L, Borghs G, Van Dorpe P. Electrical excitation of confined surface plasmon polaritons in metallic slot waveguides. Nano Lett 2010;10:1429–32.

[84] Walters RJ, van Loon RVA, Brunets I, Schmitz J, Polman A. A silicon-based electrical source of surface plasmon polaritons. Nat Mater 2010;9:21–5.
[85] Babuty A, Bousseksou A, Tetienne JP, Doyen IM, Sirtori C, Beaudoin G, Sagnes I, De Wilde Y, Colombelli R. Semiconductor surface plasmon sources. Phys Rev Lett 2010;104:226806.
[86] Wei H, Ratchford D, Li XQ, Xu HX, Shih CK. Propagating surface plasmon induced photon emission from quantum dots. Nano Lett 2009;9:4168–71.
[87] Akimov AV, Mukherjee A, Yu CL, Chang DE, Zibrov AS, Hemmer PR, Park H, Lukin MD. Generation of single optical plasmons in metallic nanowires coupled to quantum dots. Nature 2007;450:402–6.
[88] Kolesov R, Grotz B, Balasubramanian G, Stohr RJ, Nicolet AAL, Hemmer PR, Jelezko F, Wrachtrup J. Wave-particle duality of single surface plasmon polaritons. Nature Phys 2009;5:470–4.
[89] Liu SD, Cheng MT, Yang ZJ, Wang QQ. Surface plasmon propagation in a pair of metal nanowires coupled to a nanosized optical emitter. Opt Lett 2008;33:851–3.
[90] Li JH, Yu R. Single-plasmon scattering grating using nanowire surface plasmon coupled to nanodiamond nitrogen-vacancy center. Opt Express 2011;19:20991–1002.
[91] Dzsotjan D, Sorensen AS, Fleischhauer M. Quantum emitters coupled to surface plasmons of a nanowire: a Green's function approach. Phys Rev B 2010;82:075427.
[92] Kim NC, Li JB, Yang ZJ, Hao ZH, Wang QQ. Switching of a single propagating plasmon by two quantum dots system. Appl Phys Lett 2010;97:061110.
[93] Gonzalez-Tudela A, Martin-Cano D, Moreno E, Martin-Moreno L, Tejedor C, Garcia-Vidal FJ. Entanglement of two qubits mediated by one-dimensional plasmonic waveguides. Phys Rev Lett 2011;106:020501.
[94] Chen GY, Lambert N, Chou CH, Chen YN, Nori F. Surface plasmons in a metal nanowire coupled to colloidal quantum dots: scattering properties and quantum entanglement. Phys Rev B 2011;84:045310.
[95] Kolchin P, Oulton RF, Zhang X. Nonlinear quantum optics in a waveguide: distinct single photons strongly interacting at the single atom level. Phys Rev Lett 2011;106:113601.
[96] Cheng MT, Ma XS, Luo YQ, Wang PZ, Zhao GX. Entanglement generation and quantum state transfer between two quantum dot molecules mediated by quantum bus of plasmonic circuits. Appl Phys Lett 2011;99:223509.
[97] Huck A, Kumar S, Shakoor A, Anderson UL. Controlled coupling of a single nitrogen-vacancy center to a silver nanowire. Phys Rev Lett 2011;106:096801.
[98] Frimmer M, Chen YT, Koenderink AF. Scanning emitter lifetime imaging microscopy for spontaneous emission control. Phys Rev Lett 2011;107:123602.
[99] Fang YR, Wei H, Hao F, Nordlander P, Xu HX. Remote-excitation surface-enhanced raman scattering using propagating Ag nanowire plasmons. Nano Lett 2009;9:2049–53.
[100] Hutchison JA, Centeno SP, Odaka H, Fukumura H, Hofkens J, Uji-i H. Subdiffraction limited, remote excitation of surface enhanced Raman scattering. Nano Lett 2009;9: 995–1001.
[101] Fang YR, Li ZP, Huang YZ, Zhang SP, Nordlander P, Halas NJ, Xu HX. Branched silver nanowires as controllable plasmon routers. Nano Lett 2010;10:1950–4.
[102] Li ZP, Zhang SP, Halas NJ, Nordlander P, Xu HX. Coherent modulation of propagating plasmons in silver-nanowire-based structures. Small 2011;7:593–6.
[103] Wei H, Wang ZX, Tian XR, Kall M, Xu HX. Cascaded logic gates in nanophotonic plasmon networks. Nat Commun 2011;2:387.
[104] Guo X, Qiu M, Bao JM, Wiley BJ, Yang Q, Zhang XN, Ma YG, Yu HK, Tong LM. Direct coupling of plasmonic and photonic nanowires for hybrid nanophotonic components and circuits. Nano Lett 2009;9:4515–9.
[105] Pyayt AL, Wiley B, Xia YN, Chen A, Dalton L. Integration of photonic and silver nanowire plasmonic waveguides. Nature Nanotech 2008;3:660–5.
[106] Dong C-H, Ren X-F, Yang R, Duan J-Y, Guan J-G, Guo G-C, Guo G-P. Coupling of light from an optical fiber taper into silver nanowires. Appl Phys Lett 2009;95:221109.
[107] Yan RX, Pausauskie P, Huang JX, Yang PD. Direct photonic–-plasmonic coupling and routing in single nanowires. Proc Natl Acad Sci USA 2009;106:21045–50.
[108] Chen XW, Sandoghdar V, Agio M. Highly efficient interfacing of guided plasmons and photons in nanowires. Nano Lett 2009;9:3756–61.
[109] Pala RA, Shimizu KT, Melosh NA, Brongersma ML. A nonvolatile plasmonic switch employing photochromic molecules. Nano Lett 2008;8:1506–10.
[110] Dicken MJ, Sweatlock LA, Pacifici D, Lezec HJ, Bhattacharya K, Atwater HA. Electrooptic modulation in thin film barium titanate plasmonic interferometers. Nano Lett 2008;8:4048–52.
[111] Cai WS, White JS, Brongersma ML. Compact, high-speed and power-efficient electrooptic plasmonic modulators. Nano Lett 2009;9:4403–11.
[112] Dionne JA, Diest K, Sweatlock LA, Atwater HA. PlasMOStor: a metal-oxide-Si field effect plasmonic modulator. Nano Lett 2009;9:897–902.
[113] Temnov VV, Armelles G, Woggon U, Guzatov D, Cebollada A, Garcia-Martin A, Garcia-Martin JM, Thomay T, Leitenstorfer A, Bratschitsch R. Active magneto-plasmonics in hybrid metal–ferromagnet structures. Nat Photon 2010;4: 107–11.
[114] Oulton RF, Sorger VJ, Zentgraf T, Ma RM, Gladden C, Dai L, Bartal G, Zhang X. Plasmon lasers at deep subwavelength scale. Nat 2009;461:629–32.
[115] Hill MT, Marell M, Leong ESP, Smalbrugge B, Zhu Y, Sun M, van Veldhoven PJ, Geluk EJ, Karouta F, Oei Y-S, Notzel R, Ning C-Z, Smit MK. Lasing in metal-insulator-metal sub-wavelength plasmonic waveguides. Opt Express 2009;17:11107–12.
[116] Ma RM, Oulton RF, Sorger VJ, Bartal G, Zhang X. Room-temperature sub-diffraction-limited plasmon laser by total internal reflection. Nat Mater 2011;10:110–3.
[117] Wu CY, Kuo CT, Wang CY, He CL, Lin MH, Ahn H, Gwo S. Plasmonic green nanolaser based on a metal–oxide–semiconductor structure. Nano Lett 2011;11:4256–60.
[118] Berini P, De Leon I. Surface plasmon–polariton amplifiers and lasers. Nat Photon 2012;6:16–24.
[119] Peruzzo A, Laing A, Politi A, Rudolph T, O'Brien JL. Multimode quantum interference of photons in multiport integrated devices. Nat Commun 2011;2:224.
[120] Shadbolt PJ, Verde MR, Peruzzo A, Politi A, Laing A, Lobino M, Matthews JCF, Thompson MG, O'Brien JL. Generating, manipulating and measuring entanglement and mixture with a reconfigurable photonic circuit. Nat Photon 2012;6: 45–9.

Received March 9, 2012; accepted May 15, 2012